

Article

Vaginal Polyelectrolyte Layer-by-Layer Films Based on Chitosan Derivatives and Eudragit[®] S100 for pH Responsive Release of Tenofovir

Raúl Cazorla-Luna ¹, Araceli Martín-Illana ¹, Fernando Notario-Pérez ¹, Luis Miguel Bedoya ² , Aitana Tamayo ³ , Roberto Ruiz-Caro ¹, Juan Rubio ³ and María-Dolores Veiga ^{1,*}

¹ Department of Pharmaceutics and Food Technology, Faculty of Pharmacy, Complutense University of Madrid, 28040 Madrid, Spain; racazorl@ucm.es (R.C.-L.); aracelimartin@ucm.es (A.M.-I.); fnotar01@ucm.es (F.N.-P.); rruizcar@ucm.es (R.R.-C.)

² Department of Pharmacology, Pharmacognosy and Botany, Faculty of Pharmacy, Complutense University of Madrid, 28040 Madrid, Spain; lmbedoya@ucm.es

³ Institute of Ceramics and Glass, Spanish National Research Council, 28049 Madrid, Spain; aitanath@icv.csic.es (A.T.); jrubi@icv.csic.es (J.R.)

* Correspondence: mdveiga@ucm.es

Received: 11 December 2019; Accepted: 6 January 2020; Published: 9 January 2020



Abstract: Women are still at high risk of contracting the human immunodeficiency virus (HIV) virus due to the lack of protection methods under their control, especially in sub-Saharan countries. Polyelectrolyte multilayer smart vaginal films based on chitosan derivatives (chitosan lactate, chitosan tartate, and chitosan citrate) and Eudragit[®] S100 were developed for the pH-sensitive release of Tenofovir. Films were characterized through texture analysis and scanning electron microscopy (SEM). Swelling and drug release studies were carried out in simulated vaginal fluid and a mixture of simulated vaginal and seminal fluids. Ex vivo mucoadhesion was evaluated in bovine vaginal mucosa. SEM micrographs revealed the formation of multilayer films. According to texture analysis, chitosan citrate was the most flexible compared to chitosan tartrate and lactate. The swelling studies showed a moderate water uptake (<300% in all cases), leading to the sustained release of Tenofovir in simulated vaginal fluid (up to 120 h), which was accelerated in the simulated fluid mixture (4–6 h). The films had high mucoadhesion in bovine vaginal mucosa. The multilayer films formed by a mixture of chitosan citrate and Eudragit[®] S100 proved to be the most promising, with zero toxicity, excellent mechanical properties, moderate swelling (<100%), high mucoadhesion capacity, and Tenofovir release of 120 h and 4 h in vaginal fluid and the simulated fluid mixture respectively.

Keywords: chitosan lactate; chitosan tartrate; chitosan citrate; Eudragit[®] S100; layer-by-layer film; mucoadhesive film; Tenofovir controlled release; pH responsive release; vaginal preexposure prophylaxis; HIV sexual transmission

1. Introduction

Acquired immunodeficiency syndrome (AIDS) is still the leading cause of death among young women. According to United Nations Joint Programme on HIV/AIDS (UNAIDS), 460 adolescent women contract human immunodeficiency virus (HIV) each day and 350 women of the same age group die weekly of AIDS-related complications. In fact, almost 80% of people infected with HIV in the 10–19 age group in sub-Saharan Africa in 2017 were women [1]. Unfortunately, women in these countries do not benefit from options to prevent the sexual transmission of HIV such as condoms, due to gender differences which prevent them from negotiating with their sexual partners. This highlights the need to develop prevention systems that women can initiate without their partner's consent [2]. In this scenario, topical preexposure prophylaxis (PrEP) with antiretroviral drugs is one option to

prevent the sexual transmission of HIV, since they can be applied in the vagina and serve as a method of protection that can be controlled by women themselves, thus empowering them in the fight against HIV-1 infection without the consent of their sexual partner [3].

Tenofovir (TFV) is an ideal candidate for use as a topical microbicide for preventing the sexual transmission of HIV due to its efficacy, long half-life, and safety profile [4]. Clinical trials have been carried out with this drug in different dosage forms such as rings [5] and gels [6].

However, adherence is central to PrEP effectiveness, and it is essential to develop products that are easy to use and support high adherence [7]. Vaginal films are emerging as a promising option among the pharmaceutical dosage forms in developmental stages, as they are preferred over other dosage forms due to their advantages of portability, storage and handling, and also ensure comfort and ease of insertion [8,9]. Fast dissolving films based on TFV have been produced and show lower leakage and similar vaginal drug concentrations to those obtained with vaginal gels for pericoital administration. Nevertheless, sustained release formulations must be developed to provide lasting protection to women [7].

One approach to obtaining films for the sustained release of drugs is the use of the layer-by-layer (LbL) technique, which produces films composed of two or more layers of different polymers. This offers great versatility, since it combines the properties of the constituent polymers of each layer [10]. For instance, the combination of a highly mucoadhesive polymer to increase vaginal retention [11] with another polymer capable of modulating the release of the drug [12] can achieve effective and long-lasting drug release in the vaginal mucosa. The combination of polyanionic polymeric layers with polycationic polymeric layers by means of this technique also produces polyelectrolyte multilayers (PEM) [13,14], with the advantage that these polymers have a pH-dependent behaviour [15,16]. This is of great interest when developing formulations for the prevention of sexual transmission of HIV, since accelerating vaginal drug release at the time of ejaculation can increase the effectiveness of the protection [17].

Among the polycationic polymers that are being explored, chitosan is a copolymer composed of $\beta(1\rightarrow4)$ -linked 2-acetamido-2-deoxy- β -D-glucopyranose (N-acetylglucosamine) and $\alpha(1\rightarrow4)$ -linked 2-amino-2-deoxy- β -D-glucopyranose (glucosamine). Chitosan has been widely explored in the development of several pharmaceutical dosage forms such as tablets [11,18], hydrogels [19] and bigels [17], and attempts have recently been made to develop chitosan-based films as drug delivery systems [20,21]. Chitosan has mucoadhesive properties and antimicrobial activity; is from a renewable source and is completely devoid of toxicity, and has many applications in the pharmaceutical industry such as wound dressing and drug delivery systems [22,23]. This polymer has a pH-dependent solubility due to the presence of the amine groups in its structure [24], and the protonation of these groups in dilute acids allows the gelation of the polymer. Acetic acid is widely used among the various acids applied for the gelation of chitosan [25], although its strong and unpleasant smell induces rejection when applying the formulations [26]. For this reason, other acids are beginning to be used that allow the gelation of chitosan with better organoleptic properties, such as lactic acid [26], tartaric acid [27], and citric acid [28]. It has even been proven that the dilute acid used to dissolve the chitosan can condition the polymer's properties [29].

In order to improve its properties, it is possible to add suitable fillers [30,31] or combine it with different polymers such as hypromellose [32], sodium alginate [33], pectin [18], poly(vinyl alcohol) [34] and different types of Eudragit® [35,36], among which it is particularly worth highlighting Eudragit® S100 (ES100), a polyanionic copolymer derived from metacrylic acid and methyl metacrylate. It is non-soluble in acids and water but soluble in dissolutions with a pH of over 7 [37]. This behaviour makes it an interesting candidate for the development of pH-sensitive drug delivery systems for oral, ocular, vaginal and topical administration [38]. Mixtures of chitosan and ES100 have been explored with promising results, due to their ability to form polyelectrolyte complexes [39].

Although nowadays films are a promising tool for vaginal administration, the development of controlled release films is a field yet to be explored. Furthermore, the use of pH-sensitive polymers may

allow obtaining novel drug delivery systems for the prevention of sexually transmitted diseases [40]. Against this backdrop, the aim of this study is to develop PEM vaginal films based on optimized chitosan derivatives and ES100 using the LbL technique and evaluate them through scanning electron microscopy, texture analysis, swelling, ex vivo mucoadhesion and drug release tests and materials cytotoxicity. These films would allow a high mucoadhesion capacity due to the presence of the chitosan-based layer, and a sustained release in the vaginal environment thanks to the ES100 layer. After ejaculation during intercourse, the release of the drug would accelerate, thus maximizing the effectiveness of the formulations in the prevention of the sexual transmission of HIV.

2. Results and Discussion

2.1. Characterization of Chitosan Gels

The results of the characterization of the gels are shown in Figure 1.

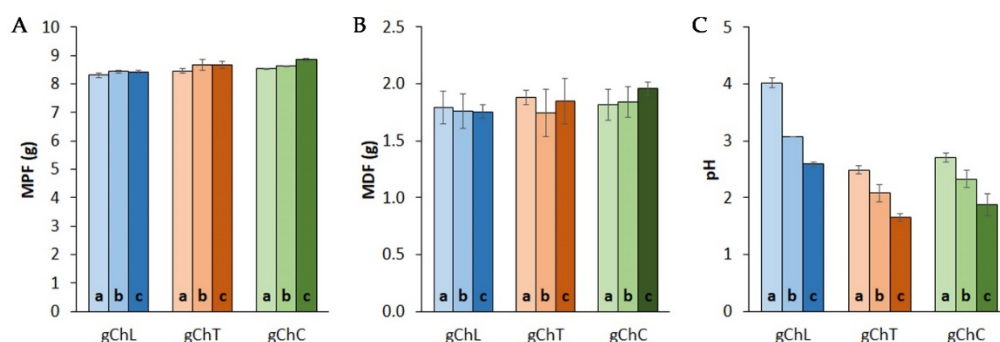


Figure 1. Results of the characterization of the chitosan gels prepared with lactic acid (gChL), tartaric acid (gChT) and citric acid (gChC) at different concentrations (0.25 M (a), 0.5 M (b) and 1 M (c)). (A) and (B) show the texture analysis results (maximum penetration force (MPF) and maximum detachment force (MDF) respectively). (C) shows the pH values obtained for the gels.

According to these data, all the gels had identical results for maximum penetration force (MPF, Figure 1A) and maximum detachment force (MDF, Figure 1B), indicating that the consistency of chitosan gels, represented by the MPF, is not modified by the acid used for its gelation. The adhesiveness of the gel, represented by the MDF, is also equal in all the gels. These properties are therefore characteristic of the polymer and are not modified by the acid. Previously published results show that pure water has similar values of MPF and MDF (7.90 ± 0.0 g and 1.49 ± 0.07 g) [41], so at these concentrations, chitosan gels have a similar consistency and adhesiveness to pure water. However, a comparison of the pH of the different gels in Figure 1C reveals some differences. In all cases an increase in the acid concentration leads to a decrease in the pH of the gel. The gels prepared with lactic acid show the highest values of pH (≈ 2.5 –4), while citric acid and tartaric acid generate more acid gels, with pH values in the range of ≈ 2 –3. According to the literature, the use of acidic substances in the vaginal environment may be beneficial for the prevention of sexually transmitted infections [42,43]. These formulations would therefore allow the acidification of the medium after administration, making them interesting candidates for the development of formulations for the prevention of sexual transmission of HIV.

2.2. Chitosan Derivative-Based Films

2.2.1. Attenuated Total Reflection Fourier Transform Infrared (FTIR-ATR) Spectroscopy

Figure 2 shows the spectra obtained for the raw materials. In the spectrum corresponding to raw chitosan, bands are observed at 1655 cm^{-1} and 1325 cm^{-1} , corresponding to the C=O bond of amide I and the N-H bond of amide III respectively. A band appears at 1585 cm^{-1} , corresponding to the free amine [44]. In the lactic acid spectrum, a peak can be observed at 1720 cm^{-1} corresponding to the C=O bond of the acid group, and a band at 1210 cm^{-1} that can be attributed to the C-O carboxylic acid bond [45]. In tartaric acid, the peak observed at 1720 cm^{-1} corresponds to the C=O bond of the

carboxylic acid. Another peak at 1445 cm^{-1} corresponds to the O-H bond of the carboxylic groups. The peaks at 1185 cm^{-1} , 3328 cm^{-1} and 3400 cm^{-1} are also attributable to O-H links [46]. In the citric acid spectrum, the peaks that appear around 1720 cm^{-1} are due to the C=O bonds of carboxylic acids. A band corresponding to the O-H bond of carboxylic acids is observed at 1390 cm^{-1} . The 3492 cm^{-1} peak is also attributable to free hydroxyls [47].

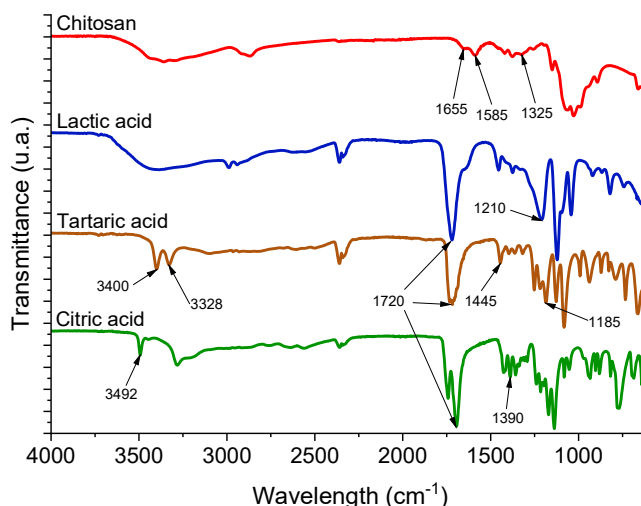


Figure 2. Spectra obtained through FTIR-ATR for the raw materials used to manufacture the chitosan derivative films.

The spectra corresponding to chitosan films prepared with different amounts of lactic acid (ChL-a, ChL-b and ChL-c) are shown in Figure 3. All have a broad band between $1660\text{--}1475\text{ cm}^{-1}$, caused by the overlapping of the chitosan amide (1655 cm^{-1}) and the C=O bond corresponding to the amide formed with lactic acid [48]. Since the carbonyl in the acid (1720 cm^{-1}) changes to amide, a reduction in the intensity of this peak can be seen in samples ChL-a and ChL-b. The peak is also observed to decrease to 1210 cm^{-1} , due to the replacement of hydroxyl in the formation of this amide (Scheme 1a). When the amount of lactic acid in the film is increased (especially in ChL-c), esters form between the lactic acid molecules, creating oligomers of polylactic acid (Scheme 1b) [48] and causing the intensity of the band to increase at 1720 cm^{-1} due to the C=O bonds corresponding to the esters. The formation of these esters is favoured by the high concentration of lactic acid, so this peak is more intense than the peak attributable to the C=O of the amide. The band at 1210 cm^{-1} also increases, indicating the presence of the C-O bond, which is absent in the amide but present in the ester [48].

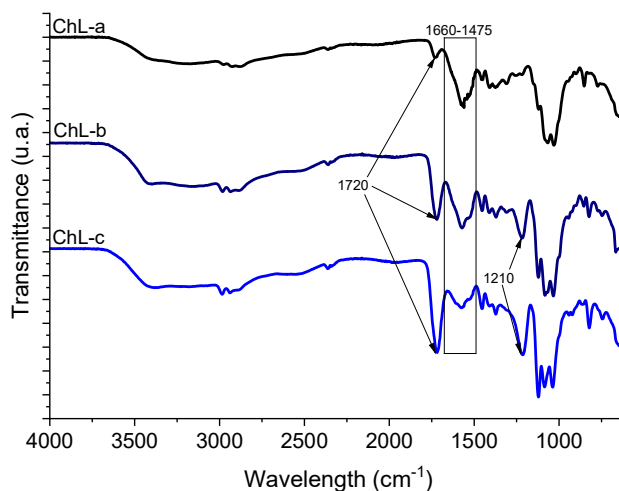
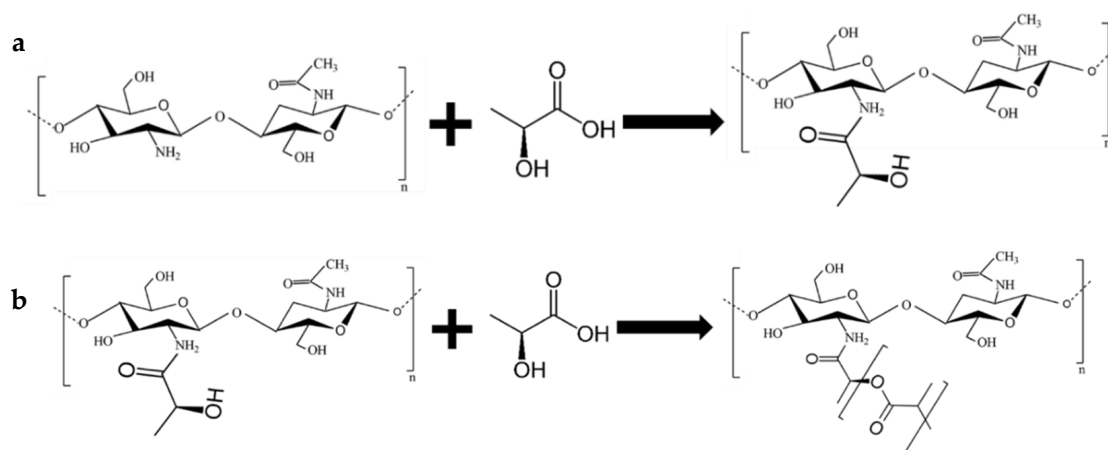


Figure 3. Spectra obtained through FTIR for the films manufactured by solvent casting chitosan gels prepared with different concentrations of lactic acid: 0.25 M (ChL-a), 0.5 M (ChL-b), and 1 M (ChL-c).



Scheme 1. Chemical reaction between chitosan and lactic acid. First, the carboxylic group of lactic acid reacts with the amine group of chitosan, forming the corresponding amide (henceforth chitosan lactate) (a). If there is an excess of lactic acid, the carboxylic groups of free molecules react with the free hydroxyl of the lactic group in chitosan lactate, forming polylactate groups (b).

The spectra corresponding to chitosan films prepared with tartaric acid are shown in Figure 4. A broad band appears between 1660 cm^{-1} and 1475 cm^{-1} , with two peaks attributable to the amide group [49]. In ChT-a and ChT-b, the peak disappears at 1445 cm^{-1} , corresponding to the O-H bond of the carboxylic acid of the tartaric acid. Other peaks that disappear with the lowest proportions of tartaric acid are 1185 cm^{-1} , 3400 cm^{-1} and 3328 cm^{-1} , which also indicates the replacement of hydroxyls in tartaric acid and confirms the formation of the amide between chitosan and tartaric acid (Scheme 2) [27]. The absence of these peaks corresponding to the O-H bonds of the carboxylic acids indicates that all acid groups react with the chitosan amines, suggesting that tartaric acid acts as a crosslinker of the chitosan chains. The peaks corresponding to O-H bonds (1445 cm^{-1} , 1185 cm^{-1} , 3328 cm^{-1} , and 3400 cm^{-1}) [46] reappear with the highest amount of tartaric acid (ChT-c), indicating that not all the tartaric acid is used in the reaction at this proportion.

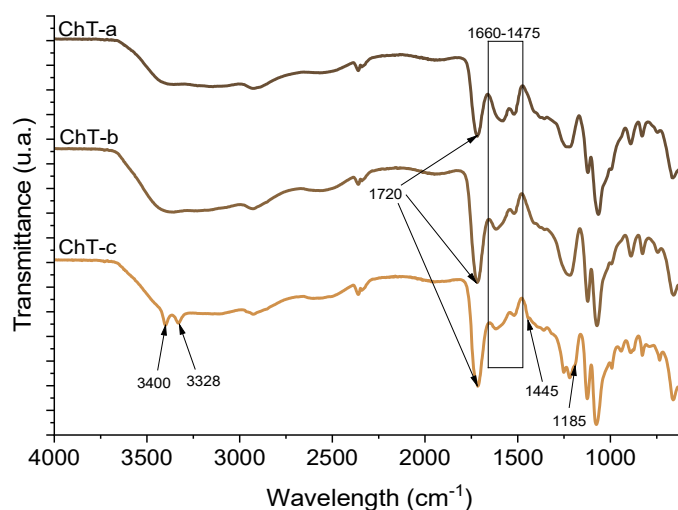
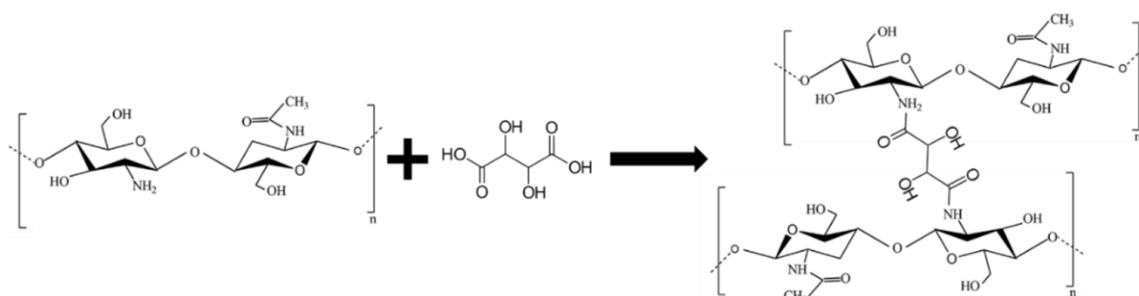


Figure 4. Spectra obtained through FTIR for the films manufactured by solvent casting chitosan gels prepared with different concentrations of tartaric acid: 0.25 M (ChT-a), 0.5 M (ChT-b) and 1 M (ChT-c).



Scheme 2. Chemical reaction between chitosan and tartaric acid. The carboxylic groups of tartaric acid react with the amine group of chitosan, forming the corresponding amide (henceforth chitosan tartrate). The complete reaction with the two carboxylic groups in the molecule of tartaric acid leads to the crosslinking of chitosan.

According to the spectra obtained for the chitosan films prepared with citric acid shown in Figure 5, a wide band appears between 1660 cm^{-1} and 1475 cm^{-1} , attributable to the formation of the amide group [50]. The bands at 1390 cm^{-1} and 3492 cm^{-1} disappear in samples ChC-a and ChC-b due to the replacement of all free carboxylic hydroxyls by the chitosan amines. This indicates that amide is formed between chitosan and citric acid, and that citric acid acts as a crosslinker for chitosan chains through an amide formed between both compounds (Scheme 3) [51]. The peaks at 1390 cm^{-1} and 3492 cm^{-1} reappear in the sample with the highest proportion of citric acid (ChC-c), suggesting that the reaction with citric acid in these proportions is incomplete.

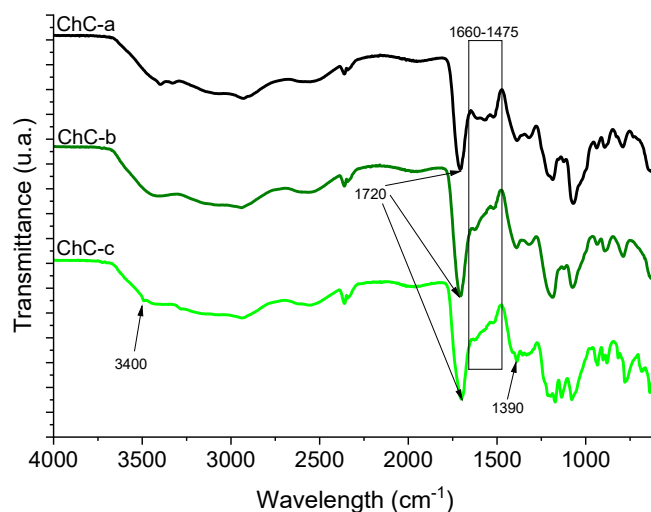
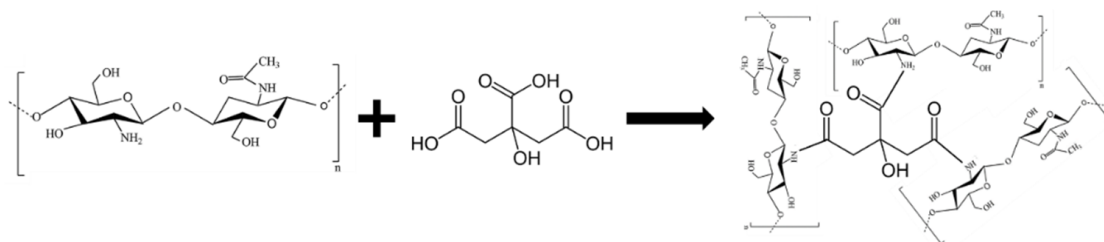


Figure 5. Spectra obtained through FTIR for the films manufactured by solvent casting chitosan gels prepared with different concentrations of citric acid: 0.25 M (ChC-a), 0.5 M (ChC-b), and 1 M (ChC-c).



Scheme 3. Chemical reaction between chitosan and citric acid. The carboxylic groups of citric acid react with the amine group of chitosan, forming the corresponding amide (henceforth chitosan citrate). The complete reaction with the three carboxylic groups in the citric acid molecule leads to the crosslinking of chitosan.

2.2.2. Appearance and Mechanical Properties

The films made with chitosan derivatives were visually evaluated. The pliability and organoleptic characteristics of each batch are shown in Table 1.

Table 1. Characteristics observed by visual evaluation of films based on chitosan derivatives.

Batch	Pliability	Organoleptic Characteristics	Comments
ChL-a	✓	Homogeneous. Translucent, yellowish and shiny. Odourless. Soft touch.	Although somewhat flexible, it breaks if folded in half.
ChL-b	✓✓	Homogeneous. Translucent, yellowish and shiny. Odourless. Soft touch.	
ChL-c	✗	Homogeneous. Translucent, yellowish and shiny. Odourless. Sticky touch.	The film can barely be handled due to its stickiness.
ChT-a	✓✓	Homogeneous. Translucent, yellowish and shiny. Odourless. Soft touch.	
ChT-b	✓✓✓	Homogeneous. Translucent, yellowish and shiny. Odourless. Soft touch.	
ChT-c	✗	Heterogeneous. Opaque, yellowish and matt. Odourless. Rough touch.	Completely rigid, it breaks when even slight force is applied.
ChC-a	✓✓	Homogeneous. Translucent, yellowish and shiny. Odourless. Soft touch.	
ChC-b	✓✓✓	Homogeneous. Translucent, yellowish and shiny. Odourless. Soft touch.	
ChC-c	✗	Heterogeneous. Opaque, yellowish and matt. Odourless. Rough touch.	Completely rigid, it breaks when even slight force is applied.

✗: Unacceptable; ✓: Acceptable; ✓✓: Good; ✓✓✓: Excellent.

The mechanical properties of the system must be taken into account when developing films for vaginal administration, as they can determine comfort and acceptability for the patient and may even be related to the performance of the film once administered. In the case of ChL-c, the formation of polylactic acid is so pronounced that the film is sticky and becomes impossible to handle. ChT-c and ChC-c films were also observed to be rigid and irregular, which can be attributed to the excess of acid during the reaction, as corroborated by FTIR studies (Section 2.2.1). The excess of tartaric acid or citric acid stiffens the film, as they are solid substances. These films were therefore discarded from further studies.

The comparison of the other films in terms of the acid used for their preparation revealed that the films with chitosan lactate had the lowest deformation capacity, while those containing chitosan tartrate or chitosan citrate had a higher capacity. This may be related to the ability of tartaric acid and citric acid to act as crosslinkers, possibly facilitating the mobility of the chitosan chains [52]. In all cases the films prepared with the diluted acids at 0.5 M (ChL-b, ChT-b, and ChC-b) were more flexible than those obtained with the diluted acids at 0.25 M (ChL-a, ChT-a, and ChC-a).

2.2.3. Drug Release Assessment

Chitosan derivative films prepared with the previously determined optimal concentration of diluted acids (ChL-b, ChT-b, ChC-b) were loaded with 30 mg of TFV (batches ChL-TFV, ChT-TFV and ChC-TFV). The drug release profiles from these chitosan derivative-based films are shown in Figure 6.

In all cases, the entire Tenofovir dose is released in 6 h, revealing the inability of these films to control the release of the drug. The crosslinking of chitosan chains generates complex three-dimensional structures, so ChC-TFV and ChT-TFV could be expected to show a greater capacity for controlled drug release than ChL-TFV, which should release the drug at the fastest rate. While this behaviour is indeed observed, there are insufficient differences between the formulations. This can be explained by

the fact that they form gels with a very low consistency, as was observed in the gel characterization studies (Section 2.1). For this reason, and to modulate the gelation rate of chitosan derivatives, and consequently the release of TFV, it was decided to prepare LbL films using ES100.

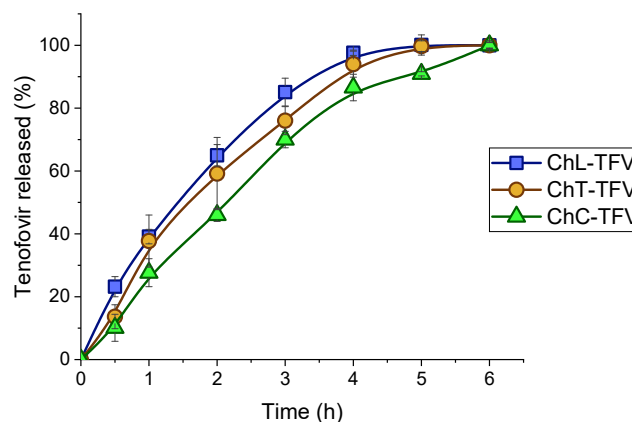


Figure 6. Tenofovir release from the films containing chitosan lactate (ChL-TFV), chitosan tartrate (ChT-TFV) and chitosan citrate (ChC-TFV).

2.3. Layer-by-Layer Films

In order to improve the properties of the chitosan derivatives, LbL films were prepared using the previously selected chitosan derivative-based films (ChL-TFV, ChT-TFV and ChC-TFV). Six different batches were obtained by adding a layer of ES100 (plasticized with Triethylcitrate (TEC)) of 75 mg (ChL/E-a, ChT/E-a and ChC/E-a) or 150 mg (ChL/E-b, ChT/E-b and ChC/E-b). As seen in the SEM micrographs (Figure 7), the layers were tightly joined and LbL films were obtained.

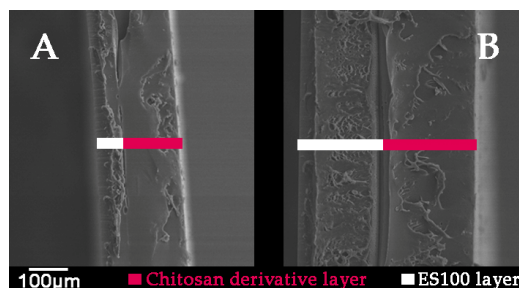


Figure 7. Micrographs of the cross-section of LbL films at 100 times magnification, with 75 mg of ES100 (A) and 150 mg of ES100 (B).

2.3.1. Texture Analysis

Figure 8 shows the deformability of the films, determined through texture analysis.

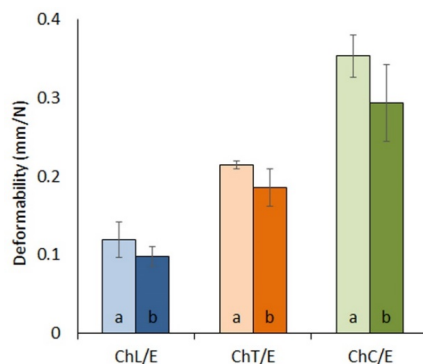


Figure 8. Results of the deformability of the LbL films containing chitosan derivatives and ES100, determined through texture analysis.

The films containing chitosan lactate (ChL/E 1 and ChL/E 2) have the lowest deformability values. Films based on chitosan tartrate (ChT/E 1 and ChT/E 2) exhibit a higher deformation capacity compared to ChL/E films. Chitosan citrate-based films (ChC/E 1 and ChC/E 2) have the highest deformability. According to the ANOVA processing, the differences are statistically significant (p -value = 1.85×10^{-11}). The proportion of ES100 also conditions the deformability of the systems with statistically significant differences (p -value = 7.73×10^{-3}), which can be attributed to the thickness of the ES100 layer. It is therefore necessary to apply a slightly greater force to obtain the same deformation when this layer is double the thickness.

These results can be explained by the fact that lactic acid is unable to crosslink chitosan chains. Conversely, tartaric acid and citric acid act as crosslinkers for chitosan, which is why these films (ChT/E and ChC/E) present better mechanical properties, as the mobility of the polymer chains may be enhanced by the presence of crosslinkers [52]. Among the films evaluated, those based on chitosan citrate (ChC/E-a and ChC/E-b) can therefore be considered to have the best mechanical properties, followed by films based on chitosan tartrate (ChT/E-a and ChT/E-b); films prepared with chitosan lactate (ChL/E-a and ChL/E-b) are the least appealing. However, all the films show good properties for handling and application, since they are highly resistant and flexible.

2.3.2. Swelling Behaviour

The results of the swelling behaviour assessment in simulated vaginal fluid (SVF) are shown in Figure 9. In the case of films based on chitosan lactate and ES100, it can be observed that the maximum amount of water imbibed is significantly greater when the ES100 layer is thicker. ChL/E-a shows a maximum swelling ratio (SR_{max}) of $\approx 200\%$ while ChL/E-b has a SR_{max} of $\approx 320\%$. The complete dissolution of the derivative (which leads to the constant weight of the formulation) occurs in both cases at 168 h. These results show a certain incompatibility between the layers, since an increase in the thickness of the ES100 layer leads to an increase in the water uptake rate and in the SR_{max} .

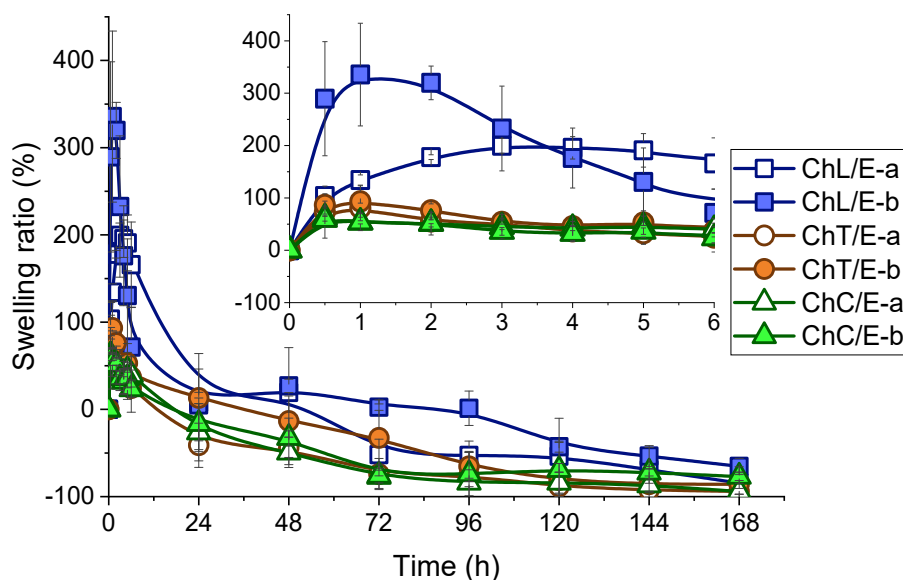


Figure 9. Swelling profiles of the LbL films in SVF.

The profiles of the batches based on chitosan tartrate (ChT/E-a, ChT/E-b) are practically overlapping, which implies that the presence of the ES100 layer does not condition the swelling process in this medium. Their low SR_{max} (less than 100%) indicate that these films swell very little. The swelling profiles of the films based on chitosan citrate and ES100 (ChC/E-a and ChC/E-b) also overlap, suggesting that the thickness of the ES100 layer does not condition the water uptake capacity, as observed in ChT/E films. These films also have the lowest SR_{max} values in SVF (less than 75%).

These results can be explained by the fact that the three-dimensional structure generated by crosslinkers in chitosan hinders water penetration [53], so although CL/E films show a higher swelling capacity, all the films could be useful for developing mucoadhesive vaginal formulations, since they swell so little that they would be extremely comfortable for the patient.

2.3.3. Ex Vivo Mucoadhesion

Ex vivo mucoadhesion was determined through texture analysis on excised bovine vaginal mucosa in SVF, and the data are shown in Figure 10. According to the results, ChL/E films have the lowest values for mucosal stickiness (represented by the work required to detach them) and adhesiveness (detachment force). This is because these films show the highest SR_{max} . According to previously published results [54], the amount of water imbibed is inversely related to the mucoadhesion capacity of a formulation, as water hinders the interaction between the polymer and the mucosa. ChT/E and ChC/E therefore show higher values for mucosal stickiness, adhesiveness or both. The results reveal that the amount of ES100 also conditions the mucoadhesion capacity of the ChT/E and ChC/E films, probably because ES100 acts as a support capable of holding the chitosan derivative. Thus the greater the amount of ES100, the greater the ability of the chitosan to bind to the mucosa. In the case of ChC/E films, the difference between the formulations points to a synergy between the layers, and shows that increasing the thickness of the ES100 layer substantially improves the mucoadhesion capacity of the chitosan derivative-based layer. Finally, it should be noted that ChC/E-b shows a slightly higher mucoadhesion capacity than ChT/E-b. The ChC/E-b film thus has a high mucoadhesion capacity, superior to the formulations previously developed, which remained mucoadhered for 120 h [18].

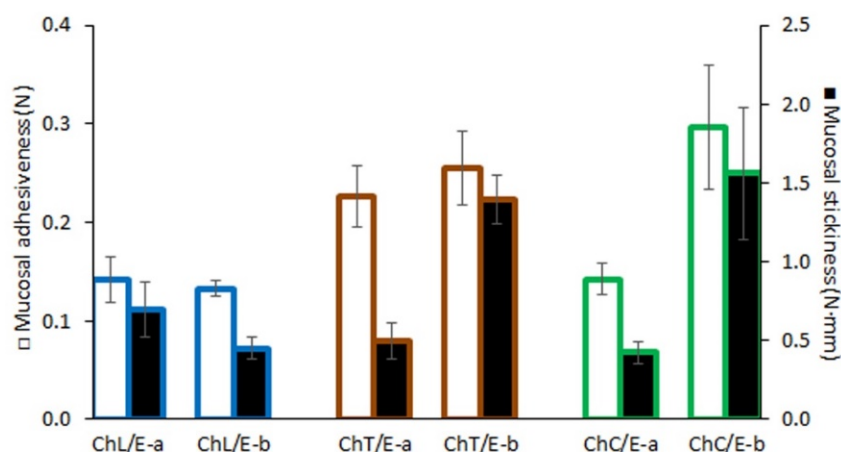


Figure 10. Ex vivo mucosal adhesiveness and stickiness obtained for the LbL films, determined in excised vaginal bovine mucosa and SVF. Mucosal adhesiveness is represented by the white bars (values on the left axis), and mucosal stickiness is by the black bars (values on the right axis).

2.3.4. Drug Release

Drug release data from the systems in SVF and SVF/SSF are shown in Figure 11. All the systems exhibited an ability to release the drug in a controlled manner in SVF (in all cases the release lasts more than 48 h), while a burst release is observed in SVF/SSF for all the systems (the complete amount of drug is released in less than 6 h).

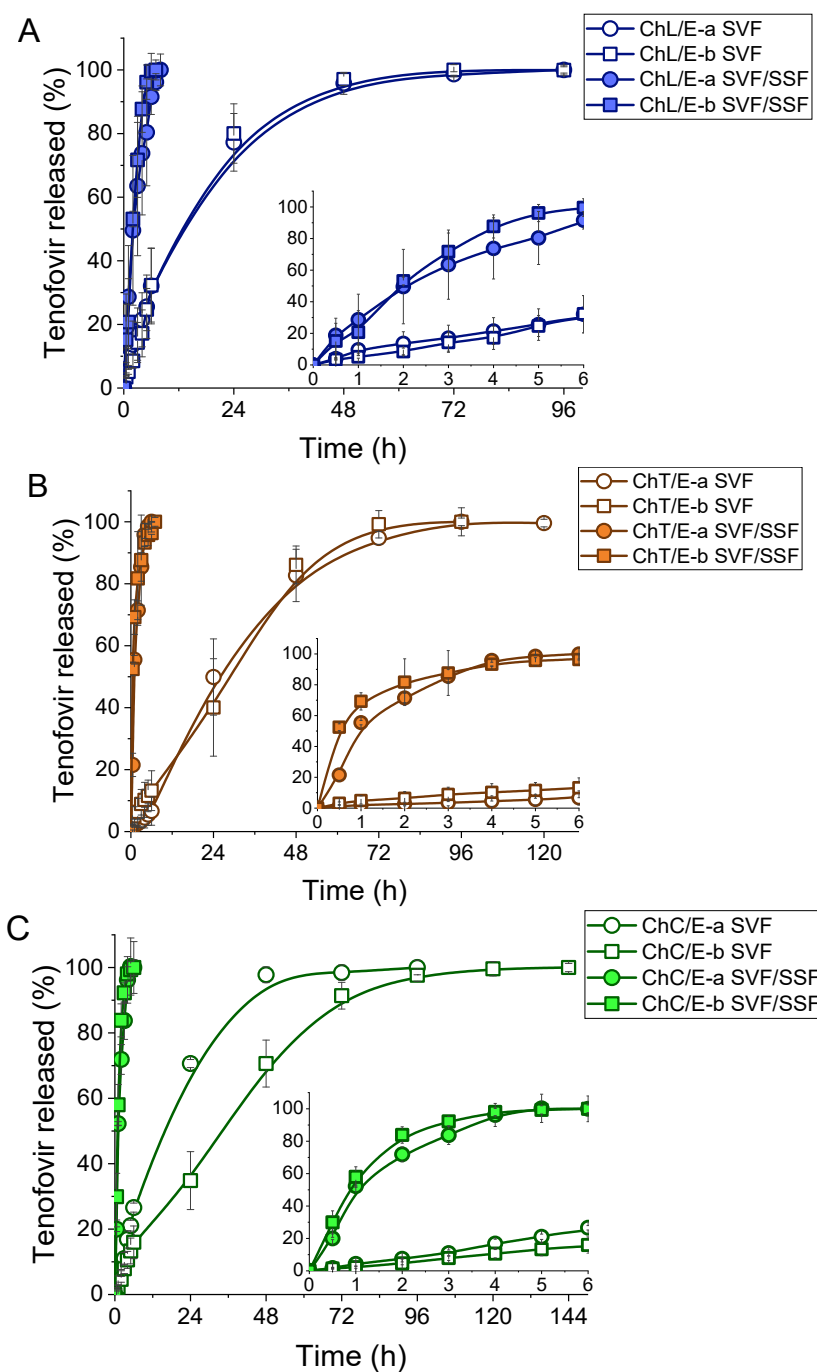


Figure 11. TFV release profiles in SVF and SVF/SSF from the LbL films based on chitosan lactate (A), chitosan tartrate (B) and chitosan citrate (C). The first 6 h of testing are amplified in the lower right corner of each graph.

According to Figure 11A, films based on chitosan lactate (ChL/E-a and ChL/E-b) show a sustained release of TFV of up to 48 h in SVF and 6 h in SVF/SSF. In films based on chitosan tartrate (ChT/E-a and ChT/E-b), whose release profiles are shown in Figure 11B, TFV release in SVF extends up to 96 h, and 4 h in SVF/SSF. In films containing chitosan citrate (ChC/E-a and ChC/E-b), the release of TFV in SVF is maintained for 120 h, while in SVF/SSF the totality of the drug is released in 4 h, as seen in Figure 11C. These findings are closely related to the swelling behaviour of LbL films, where the swelling of ChL/E-a and ChL/E-b is greater in SVF; as they have the highest penetration of water in the system, the TFV molecules are more easily accessed by the water in the medium, accelerating the drug dissolution.

The SRmax is slightly higher in ChT/E films than in ChC/E films, which explains why ChC/E films show the most extended release and also confirms that crosslinking chitosan improves the capacity to control drug release, as chitosan tartrate and chitosan citrate-based films show better controlled release than chitosan lactate-based films. A comparison of tartaric acid and citric acid suggests that citric acid is the best crosslinker and has the most persistent TFV release. However, this confirms the need for an upper layer based on ES100 to enhance the properties of the crosslinked chitosan.

According to the f_2 statistic (Table 2), no significant differences are observed in the release profiles for ChL/E and ChT/E in SVF when comparing the release from films in SVF based on the amount of ES100 in the upper layer. As seen in the swelling test results, this implies that the entry of water into the formulation is modulated by the presence of ES100 regardless of the thickness of the layer, which is key to the capacity to modulate drug release. However, ChC/E films show differences in release depending on the thickness of the ES100 layer, once again indicating a synergy between the chitosan citrate and ES100, as was observed in the mucoadhesion studies (Section 2.3.3). In SVF/SSF the entry of water is so accelerated that the difference in release based on the thickness of this layer is negligible, and they all release the drug in similar times. It is verified by statistical f_2 that the release profiles of LbL films are strongly conditioned by pH, due to the fact that ES100 is a pH-sensitive polymer that becomes soluble in aqueous media at a pH of over 7 [55]. In consequence, the dissolution of the ES100 in the medium leaves the chitosan solely responsible for the release of Tenofovir, and this polymer will release the drug in less than 8 h, as already verified in the release profiles of chitosan derivative-based films (Section 2.2.3).

Table 2. Results of f_2 processing for drug release from LbL films.

	ChL/E-a SVF	ChL/E-b SVF/SSF
ChL/E-a SVF/SSF	19.68	59.96
ChL/E-b SVF	73.63	21.21
	ChT/E-a SVF	ChT/E-b SVF/SSF
ChT/E-a SVF/SSF	14.34	34.43
ChT/E-b SVF	64.99	9.72
	ChC/E-a SVF	ChC/E-b SVF/SSF
ChC/E-a SVF/SSF	13.00	50.80
ChC/E-b SVF	43.01	11.71

The interest of this finding lies in the ability of the ChC/E-b film to offer women effective protection for a maximum of 120 h, generating a much higher concentration of TFV in the vaginal environment after ejaculation during sexual intercourse. This points to a high efficiency in the prevention of sexual transmission of HIV, and therefore justifies future evaluations.

2.4. Material Cytotoxicity

To study cell toxicity, the materials were incubated in culture media at 37 °C and 5% CO₂ for 48 h before the assay to ensure that any potential toxic component would be present in the dilutions to be tested. The cell culture was then treated with a suspension of base 5 serial dilutions of the most concentrated suspension (1000 µg/mL). Experiments were performed in lymphoblastic (MT-2) and macrophage-monocyte (THP-1) derived cell lines to evaluate toxicity on the immune cells present in vaginal or uterine mucosae, and in a uterine epithelial cell line (HEC-1A) to evaluate the potential damage to mucosal integrity (Figure 12).

As shown in Figure 12 and Table 3, lactic acid and ES100 were biocompatible in the three cell types, displaying CC₅₀ values of over 1000 µg/mL, the maximum concentration tested. Citric acid CC₅₀ value in THP-1 was around 1000 µg/mL, which is high enough to rule out a toxic effect in vivo, since it must pass through the epithelium layers at that concentration to reach the monocytes/macrophages that are

only present on the inside of the epithelium. The same can be said of TEC since its CC_{50} of around 1000 $\mu\text{g/mL}$ is only seen in MT-2 cells, which is a lymphocyte type cell line. The only compound showing cell toxicity below 1000 $\mu\text{g/mL}$ was tartaric acid, with a CC_{50} of around 200 $\mu\text{g/mL}$ in HEC-1A cells, with no effect on THP-1 and MT-2 cells. In this case tartaric acid is toxic to the epithelium cells, which could lead to the disruption of the layer and to a potential inflammatory response, facilitating viral entry through the vaginal mucosa, as other substances as nonoxynol-9 have been found to do [56]. Therefore, although the concentration needed to obtain the toxic effect is quite high (200 $\mu\text{g/mL}$), tartaric acid should be avoided in any formulation to be applied to the vaginal and/or uterine epithelium.

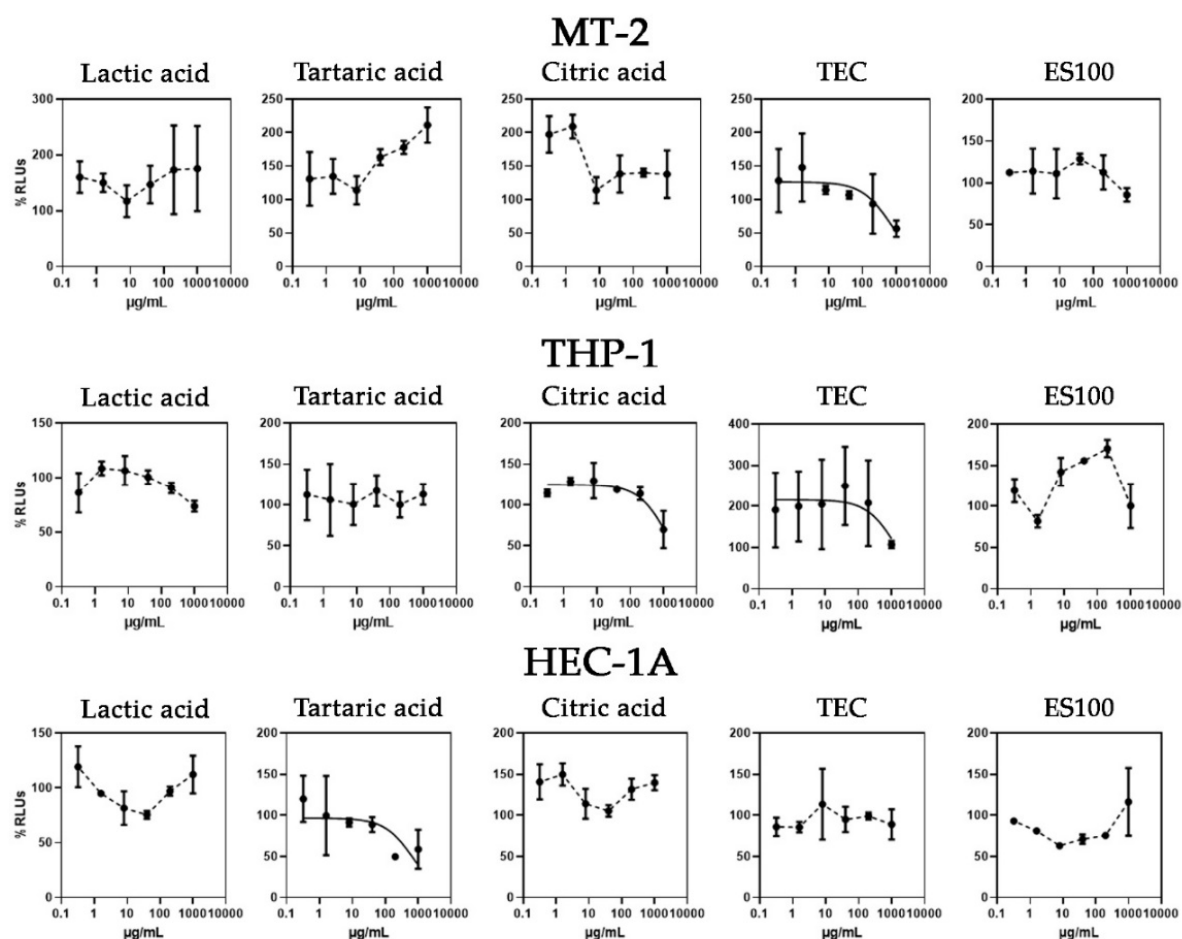


Figure 12. Graphic representation of the cytotoxic evaluation of lactic acid, tartaric acid, citric acid, TEC and ES100 in MT-2, THP-1 and HEC-1A cells. Cell viability is expressed as a percentage of living cells (%RLUs) as compared to a non-treated control (100%). RLUs: relative luminescence units.

Table 3. Results of the cytotoxicity analysis of lactic acid, tartaric acid, citric acid, TEC and ES100 in MT-2, THP-1 and HEC-1A cells. Cytotoxic concentrations 50 (CC_{50}) were calculated using GraphPad Prism software.

	CC_{50} $\mu\text{g/mL}$ (CI95%; R^2)		
	HEC-1A	THP1	MT-2
Lactic acid	>1000	>1000	>1000
Tartaric acid	≈ 200	>1000	>1000
Citric acid	>1000	≈ 1000	>1000
TEC	>1000	>1000	≈ 1000
ES100	>1000	>1000	>1000

3. Materials and Methods

3.1. Materials

Tenofovir (TFV, lot: FT104801401, MW: 287.21 g/mol, purity $\geq 98\%$) was provided by Carbosynth Limited (Berkshire, UK). Low molecular weight chitosan [18] (CH, lot: 0055790, MW ≈ 32 KDa, purity $\geq 90\%$) was supplied by Guinama (Valencia, Spain). L(+)-Lactic acid (lot: 0001552193, MW: 90.08 g/mol, purity = 90.8%) was purchased from PanReac AppliChem (Barcelona, Spain). L(+)-Tartaric acid (lot: BCBW8050, MW: 150.09 g/mol, purity = 99.97%), citric acid (lot: BCBV9045, MW: 192.12 g/mol, purity $\geq 99.5\%$) and triethylcitrate (TEC, Lot: BCBN8745V, MW: 276.28 g/mol, purity = 99.9%) were supplied by Sigma Aldrich (Saint Louis, MO, USA). Eudragit® S100 (ES100, lot: B071005090, MW = 135KDa [57]) was a kind gift from Evonik (Darmstadt, Germany). All other reagents used in this study were of analytical grade and used without further purification. Demineralized water was used in all cases.

3.2. Methods

3.2.1. Manufacture and Characterization of Chitosan Gels

Diluted acids must be used to obtain chitosan gels in aqueous media [54]. 50 mL of chitosan gels were therefore prepared with three different organic acids (lactic acid, tartaric acid and citric acid) at three concentrations, as shown in Table 4. The gels obtained were stored for 24 h at room temperature to ensure the correct hydration of the polymer, then immediately evaluated.

Table 4. Composition of the chitosan gels.

Batch	Chitosan (%)	Lactic Acid (M)	Tartaric Acid (M)	Citric Acid (M)
gChL-a	3	0.25		
gChL-b	3	0.5		
gChL-c	3	1		
gChT-a	3		0.25	
gChT-b	3		0.5	
gChT-c	3		1	
gChC-a	3			0.25
gChC-b	3			0.5
gChC-c	3			1

The influence of the acid used and its concentration on the chitosan gels was studied by evaluating their textural properties with a TA.XTplus Texture Analyser (Stable Micro Systems, Surrey, UK) using a 5 kg load cell, and following a previously described method [54]. A 20 mm-diameter stainless-steel probe with an activation force of 2 g was introduced in each gel at a rate of 0.5 mm/s to a depth of 15 mm, and returned to the initial height at the same rate. 500 points per second were monitored during data collection, and the maximum penetration force (MPF)—an accurate prediction of gel consistency—was calculated. The maximum detachment force (MDF), said to be a predictor of adhesive performance, was also recorded. The test was performed in triplicate for all the gels evaluated.

The pH of the gels was also determined using a pH-meter (GLP 21, Crison Instruments® S.A., Barcelona, Spain).

3.2.2. Chitosan Derivative-Based Films

Film Manufacture

Films were obtained from 5 mL of the previously prepared and evaluated gels using the solvent casting method [9] (Table 5) in silicon moulds. Once the solvent was completely dried at room temperature, 45-mm diameter circular films were stored until further analysis.

Table 5. Composition of the chitosan derivative films manufactured with the solvent casting method.

Batch	Chitosan (mg)	Lactic Acid (mg)	Tartaric Acid (mg)	Citric Acid (mg)	TFV (mg)
ChL-a	150	112.5 (0.25 M)			
ChL-b	150	225 (0.5 M)			
ChL-c	150	450 (1 M)			
ChT-a	150		187.5 (0.25 M)		
ChT-b	150		375 (0.5 M)		
ChT-c	150		750 (1 M)		
ChC-a	150			240 (0.25 M)	
ChC-b	150			480 (0.5 M)	
ChC-c	150			960 (1 M)	
ChL-TFV	150	225 (0.5 M)			30
ChT-TFV	150		375 (0.5 M)		30
ChC-TFV	150			480 (0.5 M)	30

The films were visually assessed to determine the optimum concentration of the different acids to obtain films based on chitosan derivatives. Their organoleptic properties were observed and their pliability was determined by folding the films, considering their capacity to deform and recover their form. The optimal proportions were then prepared using the same method with the addition of 30 mg of TFV to the gel. The amount of TFV for the development of the films was carefully selected according to literature and previous evaluations. Among the different dosage forms for the vaginal administration of this drug in clinical trials, lower and higher doses have been tested, showing adequate efficacy and security [7]. It has also been proved that extremely low cervicovaginal fluid concentration of TFV (1000 ng/mL) confer protection against HIV in women, ensuring the efficacy of these films during the release period [58]. As for the security of the films, it was confirmed in cytotoxicity studies that the dose included is not toxic for the vaginal tissue [59].

Attenuated Total Reflection Fourier Transform Infrared (FTIR-ATR) Spectroscopy

Attenuated total reflection Fourier transform infrared (FTIR-ATR) spectroscopy was used to characterize raw materials and chitosan derivative-based films with a Perkin-Elmer spectrophotometer, equipped with a MIRacle™ accessory designed for measurements (Perkin-Elmer). 16 scans were recorded for all the spectra at a resolution of 4 cm⁻¹.

Drug Release

Drug release was evaluated following the method described by Sánchez-Sánchez et al. [60]. Each sample was inserted in a borosilicate glass bottle with a 45 mm diameter base containing 80 mL of SVF and then placed in a shaking water bath (37 °C, 15 opm). Samples were taken every hour until the release of TFV was completed. 5 mL aliquots were removed and filtered, and the medium was replaced with the same volume of SVF at the same temperature. TFV concentrations were quantified by UV spectroscopy at a wavelength of 260 nm ($Abs_{SVF} = 482.05 \cdot C(\text{mg/mL}) - 0.0019$; $r^2 = 0.9996$) in an Evolution 60S spectrophotometer (Thermo Scientific, Kyoto, Japan). The test was performed in triplicate.

3.2.3. Layer-by-Layer Films

Manufacture

Although the chitosan derivative-based films had an acceptable texture, they appear unable to sufficiently modulate the release of the drug. The optimal proportions of each chitosan derivative-based film were selected to prepare LbL films, adding different proportions of ES100 to prepare the second layer (Table 6). Since ES100 is an acidic polymer, the interaction between the surface of the chitosan film and the film based on ES100 occurs through electrostatic interactions, and both layers become tightly joined. These systems were obtained using the solvent casting method. First, chitosan derivative-based

films containing TFV were prepared according to the method described above, then after the complete evaporation of water, a solution of ES100 in 10 mL acetone was added with TEC as a plasticizer. When this solvent was completely dry at room temperature, the resulting films were stored until further assessment.

Table 6. Composition of the LbL films manufactured with the solvent casting method.

		ChL/E-a	ChL/E-b	ChT/E-a	ChT/E-b	ChC/E-a	ChC/E-b
CHITOSAN DERIVATIVE-BASED LAYER	Chitosan (mg)	150	150	150	150	150	150
	Lactic acid (mg)	225	225				
	Tartaric acid (mg)			375	375		
	Citric acid (mg)					480	480
	Tenofovir (mg)	30	30	30	30	30	30
EUDRAGIT® S100-BASED LAYER	Eudragit® S100 (mg)	75	150	75	150	75	150
	Triethylcitrate (mg)	37.5	75	37.5	75	37.5	75

SEM Microscopy

To verify the structure of the film and the arrangement of the layers, the cross-sections of the films were analysed by electron microscopy using a field emission scanning electron microscope (JEOL JSM-6335F, Tokyo, Japan) at an accelerating voltage of 20 V and a work distance of 15 mm.

Texture Analysis

Although the pliability of the chitosan derivative-based films has already been assessed, the incorporation of the ES100-based layer may lead to a significant modification in the mechanical properties of the system. The texture of the LbL films was therefore evaluated according to a previously set up methodology [61] using a TA.XTplus Texture Analyser (Stable Micro Systems, Surrey, UK) with a 30 kg load cell. Before starting the experiments, each film was fixed to a support rig. A 5mm-diameter spherical stainless probe with an activation force of 5 g applied increasing force to each film to maintain a moving rate of 0.5 mm/s. 500 points per second were monitored during data collection, and the force applied (N) and the distance travelled by the probe (mm) were registered at each point. The measurement ended when the film burst at the maximum registered force. The distance travelled by the probe at the burst of the films was also recorded. The deformability of the systems was then determined as the average distance travelled by the probe when applying a force of 1 N.

All assays were performed in quadruplicate, and the data were statistically processed using two-way ANOVA (*p*-value 0.05) with the nature of the chitosan derivative and the proportion of ES100 as factors.

Swelling Behaviour

Swelling studies were performed on the LbL films to characterize the swelling of the formulations in SVF as a function of time.

The swelling processes of the different batches in SVF were analysed following the method described by Mamani et al. [62]. Fragments of each formulation with a diameter of 3 cm were fixed with cyanoacrylate adhesive to stainless steel discs of the same size, with the chitosan derivative-based layer facing the disc and the ES100 layer facing outwards, thus reproducing the expected conditions after administration. They were then placed in beakers containing 100 mL of SVF and introduced in a shaking water bath (37 °C, 15 opm). At given times (every hour during the first six hours and once a day up to constant weight), the discs were extracted from the medium and weighed after removing excess liquid. Swelling ratio (SR) was calculated according to Equation (1):

$$SR (\%) = [(F_s - F_d)/(F_d \cdot SF)] \cdot 100, \quad (1)$$

where F_s and F_d correspond to the swollen and dry film weights respectively, and SF represents the swellable fraction of the film. All the assays were performed in triplicate.

Ex Vivo Mucoadhesion

The mucoadhesion force and work were assessed ex vivo using the TA.XTplus Texture Analyser (Stable Micro Systems) to check whether the formulations show sufficient mucoadhesion capacity to adhere to the vaginal mucosa at the time of administration, using a modification of a previously described method [17]. A 2×2 cm fragment of excised bovine vaginal mucosa (obtained from a local slaughterhouse) was fixed to the bottom of a Petri dish and hydrated with 5 mL of SVF. The LbL film was fixed to a 1 cm-diameter cylindrical probe, with the chitosan derivative layer facing the vaginal mucosa, as expected at the time of administration. The preparation was moved at a speed of 1 mm/s until it came into contact with the vaginal mucosa, applying a contact force of 500 g for 30 s. The probe was then separated from the sample at a speed of 1 mm/s up to the starting height of the test. The maximum force required to separate the film from the vaginal mucosa (detachment force) was recorded as the mucosal adhesiveness. The area under the curve between the force-distance profiles (detachment work) was determined, which is considered to be the mucosal stickiness. Each batch was evaluated in triplicate.

Drug Release

To verify that the release of TFV from the films is pH dependent, the drug release from the LbL films was evaluated in SVF (pH = 4.2) and in a SVF and simulated seminal fluid mixture (SVF/SSF, ratio 1:4, pH = 7.5 [63]) to reproduce the conditions after ejaculation during intercourse. Each sample was inserted in a borosilicate glass bottle with a 45-mm diameter base containing 80 mL of medium, with the hydrophilic layer of the film in contact with the glass and the hydrophobic layer in contact with the medium, as it would be positioned in the vagina. The preparation was then placed in a shaking water bath (37 °C, 15 rpm). Samples were taken every hour during the first six hours and every day after that at given times. 5 mL aliquots were removed and filtered, and the medium was replaced with the same volume of either SVF or SVF/SSF at the same temperature. TFV concentrations were quantified by UV spectroscopy at a wavelength of 260 nm ($Abs_{SVF/SSF} = 482.23 \cdot C(\text{mg/mL}) - 0.0145$; $r^2 = 0.9990$) in an Evolution 60S spectrophotometer (Thermo Scientific, Kyoto, Japan). The test was performed in triplicate.

The release profiles of the LbL films were compared using a f_2 statistic [64] in order to determine whether there are significant differences between the two media, and whether the thickness of the ES100 layer determines the release of the drug.

3.2.4. Material Cytotoxicity

Three human cell lines were used: a lymphoblastic cell line, MT-2 [65], a macrophage-monocyte derived cell line, THP-1 (ATCC® TIB-202) and a uterine/endometrial epithelial cell line, HEC-1A (ATCC® HTB-112™) (kindly provided by Maria Angeles Muñoz). All the cell lines were cultured in RPMI 1640 medium supplemented with 10 % (*v/v*) fetal bovine serum, 2 mM L-glutamine and 50 mg/mL streptomycin (all Whittaker M.A. Bio-Products, Walkerville, MD, USA) at 37 °C in a humidified atmosphere of 5 % CO₂. To detach the HEC-1-A cells, the medium was removed and the flask was rinsed during 10 min with 1 to 2 mL of trypsin 0.25%—EDTA 0.03% solution. The medium was replaced every three days after cell centrifugation at 1500 rpm for 5 min.

Cell toxicity was measured using the CellTiter Glo kit (Promega, Madison, WI, USA). Cells were incubated in 96-well plates at a density of 10×10^5 cells per well (MT-2 and THP-1) and 2×10^4 (HEC-1A) in complete medium. To assess the cytotoxic effect, cells were exposed to fresh medium containing different concentrations of lactic acid, tartaric acid, citric acid, TEC and ES100 suspensions, or the same concentration of PBS 1× as control. Experiments were performed in triplicate and the culture was maintained at 37 °C and 5% CO₂ humidified atmosphere for 48 h. A standard method was

followed to suspend the materials in PBS 1× [66]. After incubation for 48 h, the medium was removed from cell cultures and 50 µL of CellTiter Glo reactive was added to each well on the plate. Relative luminescence units (RLUs) were measured in a luminometer (Sirius, Berthold Detection Systems). Cytotoxic concentration 50 (CC₅₀) values were calculated using GraphPad Prism Software (non-linear regression, log inhibitor versus response). The results of the cytotoxic assay are shown as the average of at least three individual experiments.

4. Conclusions

The gelation of chitosan in different diluted acids allows the production of chitosan derivative-based films with different mechanical properties without the need to include plasticizers. It has been confirmed that the crosslinking of the chitosan chains with tartaric acid or citric acid generates films with improved mechanical properties. The combination of these films with a polymer with pH-sensitive solubility (Eudragit® S100) produces formulations that exhibit a pH-dependant Tenofovir release, high mucoadhesion, and a moderate swelling profile, which would make them comfortable for the patient.

Among the films obtained through the layer-by-layer technique, those based on the combination of chitosan citrate and Eudragit® S100 in a 1:1 ratio (ChC/E-b) allow a sustained release of Tenofovir for up to five days in simulated vaginal fluid and release all the drug in less than 4 h after sexual intercourse, with very moderate swelling and a high mucoadhesion capacity. The materials used were also non-toxic in the vaginal environment. These formulations are thus a future option for the prevention of the sexual transmission of HIV in women.

Author Contributions: Conceptualization, R.C.-L., R.R.-C., and M.-D.V.; Funding acquisition, M.-D.V.; Investigation, R.C.-L., A.M.-I., F.N.-P., L.M.B. and A.T.; Methodology, R.C.-L., R.R.-C., J.R. and M.-D.V.; Project administration, R.R.-C., and M.-D.V.; Supervision, J.R., R.R.-C., and M.-D.V.; Writing—original draft, R.C.-L.; Writing—review & editing, M.-D.V., and R.R.-C. All authors have read and agreed to the published version of the manuscript.

Funding: This work was supported by project MAT2016-76416-R financed by the Spanish Research Agency and the European Regional Development Fund (AEI/FEDER, UE).

Acknowledgments: Raúl Cazorla-Luna and Araceli Martín-Illana are beneficiaries of university professor training fellowships granted by the Spanish Ministry of Education, Culture and Sport. Fernando Notario-Pérez is the beneficiary of a research training fellowship granted by the Spanish Ministry of Science, Innovation and Universities. We are grateful to the Carnes Barbero slaughterhouse (El Barraco, Ávila, Spain) for supplying the bovine vaginal mucosa samples. We would also like to thank María Hernando, veterinarian of the Junta de Castilla y León, for verifying the suitability of these biological samples. Scanning electron microscopy was done at the National Electron Microscopy Centre, part of the Research Support Centres and Unique Science and Technology Facility at the Complutense University of Madrid.

Conflicts of Interest: The authors declare no conflict of interest.

References

1. United Nations Joint Programme on HIV/AIDS (UNAIDS). *On International Women's Day, UNAIDS Calls for Greater Action to Protect Young Women and Adolescent Girls*; United Nations Joint Programme on HIV/AIDS (UNAIDS): Geneva, Switzerland, 2019.
2. Stankevitz, K.; Schwartz, K.; Hoke, T.; Li, Y.; Lanham, M.; Mahaka, I.; Mullick, S. Reaching at-risk women for PrEP delivery: What can we learn from clinical trials in sub-Saharan Africa? *PLoS ONE* **2019**, *14*, e0218556. [[CrossRef](#)] [[PubMed](#)]
3. Yang, H.; Li, J.; Patel, S.K.; Palmer, K.E.; Devlin, B.; Rohan, L.C. Design of Poly(lactic-co-glycolic Acid) (PLGA) Nanoparticles for Vaginal Co-Delivery of Griffithsin and Dapivirine and Their Synergistic Effect for HIV Prophylaxis. *Pharmaceutics* **2019**, *11*, 184. [[CrossRef](#)]
4. McConville, C.; Boyd, P.; Major, I. Efficacy of Tenofovir 1% Vaginal Gel in Reducing the Risk of HIV-1 and HSV-2 Infection. *Clin. Med. Insights Women's Heal.* **2014**, *7*, 1–8. [[CrossRef](#)]

5. Thurman, A.R.; Schwartz, J.L.; Brache, V.; Clark, M.R.; McCormick, T.; Chandra, N.; Marzinke, M.A.; Stanczyk, F.Z.; Dezzutti, C.S.; Hillier, S.L.; et al. Randomized, placebo controlled phase I trial of safety, pharmacokinetics, pharmacodynamics and acceptability of tenofovir and tenofovir plus levonorgestrel vaginal rings in women. *PLoS ONE* **2018**, *13*, e0199778. [[CrossRef](#)]
6. Delany-Moretlwe, S.; Lombard, C.; Baron, D.; Bekker, L.-G.; Nkala, B.; Ahmed, K.; Sebe, M.; Brumskine, W.; Nchabeleng, M.; Palanee-Philips, T.; et al. Tenofovir 1% vaginal gel for prevention of HIV-1 infection in women in South Africa (FACTS-001): A phase 3, randomised, double-blind, placebo-controlled trial. *Lancet Infect. Dis.* **2018**, *18*, 1241–1250. [[CrossRef](#)]
7. Marzinke, M.A.; Moncla, B.J.; Hendrix, C.W.; Richardson-Harman, N.; Dezzutti, C.S.; Schwartz, J.L.; Spiegel, H.M.L.; Hillier, S.L.; Bunge, K.E.; Meyn, L.A.; et al. FAME-04: A Phase 1 trial to assess the safety, acceptability, pharmacokinetics and pharmacodynamics of film and gel formulations of tenofovir. *J. Int. AIDS Soc.* **2018**, *21*, e25156.
8. Jalil, A.; Asim, M.H.; Le, N.-M.N.; Laffleur, F.; Matuszczak, B.; Tribus, M.; Bernkop-Schnürch, A. S-protected gellan gum: Decisive approach towards mucoadhesive antimicrobial vaginal films. *Int. J. Biol. Macromol.* **2019**, *130*, 148–157. [[CrossRef](#)]
9. Machado, R.M.; Palmeira-De-Oliveira, A.; Martinez-De-Oliveira, J.; Palmeira-De-Oliveira, R. Vaginal films for drug delivery. *J. Pharm. Sci.* **2013**, *102*, 2069–2081. [[CrossRef](#)]
10. Guzmán, E.; Mateos-Maroto, A.; Ruano, M.; Ortega, F.; Rubio, R.G. Layer-by-Layer polyelectrolyte assemblies for encapsulation and release of active compounds. *Adv. Colloid Interface Sci.* **2017**, *249*, 290–307. [[CrossRef](#)]
11. Notario-Pérez, F.; Martín-Illana, A.; Cazorla-Luna, R.; Ruiz-Caro, R.; Peña, J.; Veiga, M.D. Improvement of Tenofovir vaginal release from hydrophilic matrices through drug granulation with hydrophobic polymers. *Eur. J. Pharm. Sci.* **2018**, *117*, 204–215. [[CrossRef](#)]
12. Melegari, C.; Bertoni, S.; Genovesi, A.; Hughes, K.; Rajabi-Siahboomi, A.R.; Passerini, N.; Albertini, B. Ethylcellulose film coating of guaifenesin-loaded pellets: A comprehensive evaluation of the manufacturing process to prevent drug migration. *Eur. J. Pharm. Biopharm.* **2016**, *100*, 15–26. [[CrossRef](#)]
13. Volodkin, D.; von Klitzing, R. Competing mechanisms in polyelectrolyte multilayer formation and swelling: Polycation–polyanion pairing vs. polyelectrolyte–ion pairing. *Curr. Opin. Colloid Interface Sci.* **2014**, *19*, 25–31. [[CrossRef](#)]
14. Jeganathan, B.; Prakya, V.; Deshmukh, A. Preparation and Evaluation of Diclofenac Sodium Tablet Coated with Polyelectrolyte Multilayer Film Using Hypromellose Acetate Succinate and Polymethacrylates for pH-Dependent, Modified Release Drug Delivery. *AAPS PharmSciTech* **2016**, *17*, 578–587. [[CrossRef](#)]
15. Lokova, A.Y.; Zaborova, O.V. Modification of liposomes with a polycation can enhance the control of pH-induced release. *Int. J. Nanomed.* **2019**, *14*, 1039–1049. [[CrossRef](#)]
16. Wang, X.-Q.; Zhang, Q. pH-sensitive polymeric nanoparticles to improve oral bioavailability of peptide/protein drugs and poorly water-soluble drugs. *Eur. J. Pharm. Biopharm.* **2012**, *82*, 219–229. [[CrossRef](#)]
17. Martín-Illana, A.; Notario-Pérez, F.; Cazorla-Luna, R.; Ruiz-Caro, R.; Veiga, M.D. Smart Freeze-Dried Bigels for the Prevention of the Sexual Transmission of HIV by Accelerating the Vaginal Release of Tenofovir during Intercourse. *Pharmaceutics* **2019**, *11*, 232. [[CrossRef](#)]
18. Cazorla-Luna, R.; Notario-Pérez, F.; Martín-Illana, A.; Tamayo, A.; Rubio, J.; Ruiz-Caro, R.; Veiga, M.D. Chitosan-Based Mucoadhesive Vaginal Tablets for Controlled Release of the Anti-HIV Drug Tenofovir. *Pharmaceutics* **2019**, *11*, 20. [[CrossRef](#)]
19. Frank, L.A.; Sandri, G.; D’Autilia, F.; Contri, R.V.; Bonferoni, M.C.; Caramella, C.; Frank, A.G.; Pohlmann, A.R.; Guterres, S.S. Chitosan gel containing polymeric nanocapsules: A new formulation for vaginal drug delivery. *Int. J. Nanomedicine* **2014**, *9*, 3151. [[PubMed](#)]
20. Kilicarslan, M.; Ilhan, M.; Inal, O.; Orhan, K. Preparation and evaluation of clindamycin phosphate loaded chitosan/alginate polyelectrolyte complex film as mucoadhesive drug delivery system for periodontal therapy. *Eur. J. Pharm. Sci.* **2018**, *123*, 441–451. [[CrossRef](#)] [[PubMed](#)]
21. Layek, B.; Rahman Nirzhor, S.S.; Rath, S.; Kandimalla, K.K.; Wiedmann, T.S.; Prabha, S. Design, Development, and Characterization of Imiquimod-Loaded Chitosan Films for Topical Delivery. *AAPS PharmSciTech* **2019**, *20*, 58. [[CrossRef](#)]
22. Ali, A.; Ahmed, S. A review on chitosan and its nanocomposites in drug delivery. *Int. J. Biol. Macromol.* **2018**, *109*, 273–286. [[CrossRef](#)] [[PubMed](#)]

23. Valenta, C. The use of mucoadhesive polymers in vaginal delivery. *Adv. Drug Deliv. Rev.* **2005**, *57*, 1692–1712. [[CrossRef](#)] [[PubMed](#)]
24. Cheung, R.C.F.; Ng, T.B.; Wong, J.H.; Chan, W.Y. Chitosan: An Update on Potential Biomedical and Pharmaceutical Applications. *Mar. Drugs* **2015**, *13*, 5156–5186. [[CrossRef](#)] [[PubMed](#)]
25. Furuike, T.; Komoto, D.; Hashimoto, H.; Tamura, H. Preparation of chitosan hydrogel and its solubility in organic acids. *Int. J. Biol. Macromol.* **2017**, *104*, 1620–1625. [[CrossRef](#)]
26. Soares, L.S.; Perim, R.B.; de Alvarenga, E.S.; Guimarães, L.M.; Teixeira, A.V.N.C.; Coimbra, J.S.D.R.; de Oliveira, E.B. Insights on physicochemical aspects of chitosan dispersion in aqueous solutions of acetic, glycolic, propionic or lactic acid. *Int. J. Biol. Macromol.* **2019**, *128*, 140–148. [[CrossRef](#)]
27. Tronci, G.; Ajiro, H.; Russell, S.J.; Wood, D.J.; Akashi, M. Tunable drug-loading capability of chitosan hydrogels with varied network architectures. *Acta Biomater.* **2014**, *10*, 821–830. [[CrossRef](#)]
28. Libio, I.C.; Demori, R.; Ferrão, M.F.; Lionzo, M.I.Z.; da Silveira, N.P. Films based on neutralized chitosan citrate as innovative composition for cosmetic application. *Mater. Sci. Eng. C* **2016**, *67*, 115–124. [[CrossRef](#)]
29. Stie, M.B.; Jones, M.; Sørensen, H.O.; Jacobsen, J.; Chronakis, I.S.; Nielsen, H.M. Acids ‘generally recognized as safe’ affect morphology and biocompatibility of electrospun chitosan/polyethylene oxide nanofibers. *Carbohydr. Polym.* **2019**, *215*, 253–262. [[CrossRef](#)]
30. Benucci, I.; Liburdi, K.; Cacciotti, I.; Lombardelli, C.; Zappino, M.; Nanni, F.; Esti, M. Chitosan/clay nanocomposite films as supports for enzyme immobilization: An innovative green approach for winemaking applications. *Food Hydrocoll.* **2018**, *74*, 124–131. [[CrossRef](#)]
31. Cacciotti, I.; Lombardelli, C.; Benucci, I.; Esti, M. Clay/chitosan biocomposite systems as novel green carriers for covalent immobilization of food enzymes. *J. Mater. Res. Technol.* **2019**, *8*, 3644–3652. [[CrossRef](#)]
32. Notario-Pérez, F.; Cazorla-Luna, R.; Martín-Illana, A.; Ruiz-Caro, R.; Tamayo, A.; Rubio, J.; Veiga, M.D. Optimization of tenofovir release from mucoadhesive vaginal tablets by polymer combination to prevent sexual transmission of HIV. *Carbohydr. Polym.* **2018**, *179*, 305–316. [[CrossRef](#)] [[PubMed](#)]
33. Kyzioł, A.; Mazgała, A.; Michna, J.; Regiel-Futyr, A.; Sebastian, V. Preparation and characterization of alginate/chitosan formulations for ciprofloxacin-controlled delivery. *J. Biomater. Appl.* **2017**, *32*, 162–174. [[CrossRef](#)]
34. Ali, A.; Shahid, M.A.; Hossain, M.D.; Islam, M.N. Antibacterial bi-layered polyvinyl alcohol (PVA)-chitosan blend nanofibrous mat loaded with Azadirachta indica (neem) extract. *Int. J. Biol. Macromol.* **2019**, *138*, 13–20. [[CrossRef](#)]
35. Ubaid, M.; Shah, S.N.H.; Khan, S.A.; Murtaza, G. Synthesis and Characterization of pH-Sensitive Genipin Cross-Linked Chitosan/Eudragit® L100 Hydrogel for Metformin Release Study Using Response Surface Methodology. *Curr. Drug Deliv.* **2018**, *15*, 1343–1358. [[CrossRef](#)] [[PubMed](#)]
36. Chen, S.; Guo, F.; Deng, T.; Zhu, S.; Liu, W.; Zhong, H.; Yu, H.; Luo, R.; Deng, Z. Eudragit S100-Coated Chitosan Nanoparticles Co-loading Tat for Enhanced Oral Colon Absorption of Insulin. *AAPS PharmSciTech* **2017**, *18*, 1277–1287. [[CrossRef](#)] [[PubMed](#)]
37. Ansari, F.; Pourjafar, H.; Jodat, V.; Sahebi, J.; Ataei, A. Effect of Eudragit S100 nanoparticles and alginate chitosan encapsulation on the viability of Lactobacillus acidophilus and Lactobacillus rhamnosus. *AMB Express* **2017**, *7*, 144. [[CrossRef](#)]
38. Qindeel, M.; Ahmed, N.; Sabir, F.; Khan, S.; Ur-Rehman, A. Development of novel pH-sensitive nanoparticles loaded hydrogel for transdermal drug delivery. *Drug Dev. Ind. Pharm.* **2019**, *45*, 629–641. [[CrossRef](#)]
39. Prasad, S.; Dangi, J.S. Development and characterization of pH responsive polymeric nanoparticles of SN-38 for colon cancer. *Artif. Cells Nanomed. Biotechnol.* **2016**, *44*, 1824–1834. [[CrossRef](#)]
40. Solanki, A.; Thakore, S. Cellulose crosslinked pH-responsive polyurethanes for drug delivery: α -hydroxy acids as drug release modifiers. *Int. J. Biol. Macromol.* **2015**, *80*, 683–691. [[CrossRef](#)]
41. Martín-illana, A.; Cazorla-luna, R.; Notario-pérez, F.; Bedoya, L.M.; Ruiz-caro, R.; Dolores, M. Freeze-dried bioadhesive vaginal bigels for controlled release of Tenofovir. *Eur. J. Pharm. Sci.* **2019**, *127*, 38–51. [[CrossRef](#)]
42. Nelson, A.L. An overview of properties of Amphora (Acidform) contraceptive vaginal gel. *Expert Opin. Drug Saf.* **2018**, *17*, 935–943. [[CrossRef](#)] [[PubMed](#)]
43. Notario-Pérez, F.; Ruiz-Caro, R.; Veiga-Ochoa, M.D. Historical development of vaginal microbicides to prevent sexual transmission of HIV in women: From past failures to future hopes. *Drug Des. Devel. Ther.* **2017**, *11*, 1767–1787. [[CrossRef](#)] [[PubMed](#)]

44. Benucci, I.; Lombardelli, C.; Cacciotti, I.; Liburdi, K.; Nanni, F.; Esti, M. Chitosan beads from microbial and animal sources as enzyme supports for wine application. *Food Hydrocoll.* **2016**, *61*, 191–200. [\[CrossRef\]](#)
45. Kowalczyk, D.; Kordowska-Wiater, M.; Nowak, J.; Baraniak, B. Characterization of films based on chitosan lactate and its blends with oxidized starch and gelatin. *Int. J. Biol. Macromol.* **2015**, *77*, 350–359. [\[CrossRef\]](#)
46. Izutsu, H.; Mizukami, F.; Kiyozumi, Y.; Maeda, K. Preparation and characterization of L-tartaric acid–silica composites recognizing molecular asymmetry. *J. Mater. Chem.* **1997**, *7*, 1519–1525. [\[CrossRef\]](#)
47. Lin, H.; Su, J.; Kankala, R.K.; Zeng, M.; Zhou, S.-F.; Lin, X. Using pH-Activable Carbon Nanoparticles as Cell Imaging Probes. *Micromachines* **2019**, *10*, 568. [\[CrossRef\]](#)
48. Bhattarai, N.; Ramay, H.R.; Chou, S.H.; Zhang, M. Chitosan and lactic acid-grafted chitosan nanoparticles as carriers for prolonged drug delivery. *Int. J. Nanomed.* **2006**, *1*, 181–187. [\[CrossRef\]](#)
49. Basumallick, S.; Gabriela Nogueira Campos, M.; Richardson, D.; Gesquiere, A.; Santra, S. Hydrothermally treated chitosan spontaneously forms water-soluble spherical particles stable at a wide pH range. *Int. J. Polym. Mater. Polym. Biomater.* **2016**, *65*, 751–758. [\[CrossRef\]](#)
50. Gyllenè, O.; Nivinskienè, O.; Vengris, T. Sorption of tartrate, citrate, and EDTA onto chitosan and its regeneration applying electrolysis. *Carbohydr. Res.* **2008**, *343*, 1324–1332. [\[CrossRef\]](#)
51. Bagheri, M.; Younesi, H.; Hajati, S.; Borghei, S.M. Application of chitosan-citric acid nanoparticles for removal of chromium (VI). *Int. J. Biol. Macromol.* **2015**, *80*, 431–444. [\[CrossRef\]](#)
52. Miles, K.B.; Ball, R.L.; Matthew, H.W.T. Chitosan films with improved tensile strength and toughness from N-acetyl-cysteine mediated disulfide bonds. *Carbohydr. Polym.* **2016**, *139*, 1–9. [\[CrossRef\]](#) [\[PubMed\]](#)
53. Xu, S.; Li, H.; Ding, H.; Fan, Z.; Pi, P.; Cheng, J.; Wen, X. Allylated chitosan-poly(N-isopropylacrylamide) hydrogel based on a functionalized double network for controlled drug release. *Carbohydr. Polym.* **2019**, *214*, 8–14. [\[CrossRef\]](#) [\[PubMed\]](#)
54. Cazorla-Luna, R.; Martín-Illana, A.; Notario-Pérez, F.; Bedoya, L.-M.; Bermejo, P.; Ruiz-Caro, R.; Veiga, M.-D. Dapivirine Bioadhesive Vaginal Tablets Based on Natural Polymers for the Prevention of Sexual Transmission of HIV. *Polymers (Basel)* **2019**, *11*, 483. [\[CrossRef\]](#) [\[PubMed\]](#)
55. Mehta, R.; Chawla, A.; Sharma, P.; Pawar, P. Formulation and in vitro evaluation of Eudragit S-100 coated naproxen matrix tablets for colon-targeted drug delivery system. *J. Adv. Pharm. Technol. Res.* **2019**, *4*, 31–41.
56. Wilkinson, D.; Ramjee, G.; Tholandi, M.; Rutherford, G.W. Nonoxynol-9 for preventing vaginal acquisition of HIV infection by women from men. *Cochrane Database Syst. Rev.* **2002**, *4*, CD003939. [\[CrossRef\]](#)
57. Ai, Z.; Jiang, Z.; Li, L.; Deng, W.; Kusakabe, I.; Li, H. Immobilization of *Streptomyces olivaceoviridis* E-86 xylanase on Eudragit S-100 for xylo-oligosaccharide production. *Process Biochem.* **2005**, *40*, 2707–2714. [\[CrossRef\]](#)
58. Moss, J.A.; Malone, A.M.; Smith, T.J.; Butkyavichene, I.; Cortez, C.; Gilman, J.; Kennedy, S.; Kopin, E.; Nguyen, C.; Sinha, P.; et al. Safety and pharmacokinetics of intravaginal rings delivering tenofovir in pig-tailed macaques. *Antimicrob. Agents Chemother.* **2012**, *56*, 5952–5960. [\[CrossRef\]](#)
59. Notario-Pérez, F.; Martín-Illana, A.; Cazorla-Luna, R.; Ruiz-Caro, R.; Bedoya, L.M.; Tamayo, A.; Rubio, J.; Veiga, M.D. Influence of chitosan swelling behaviour on controlled release of tenofovir from mucoadhesive vaginal systems for prevention of sexual transmission of HIV. *Mar. Drugs* **2017**, *15*, 50. [\[CrossRef\]](#)
60. Bermejo, P.; Rubio, J.; Martín-Illana, A.; Sánchez-Sánchez, M.-P.; Bedoya, L.-M.; Otero-Espinar, F.; Fernández-Ferreiro, A.; Carro, R.; Veiga, M.-D.; Ruiz-Caro, R.; et al. Chitosan and Kappa-Carrageenan Vaginal Acyclovir Formulations for Prevention of Genital Herpes. In Vitro and Ex Vivo Evaluation. *Mar. Drugs* **2015**, *13*, 5976–5992.
61. Notario-Pérez, F.; Martín-Illana, A.; Cazorla-Luna, R.; Ruiz-Caro, R.; Bedoya, L.-M.; Peña, J.; Veiga, M.-D. Development of mucoadhesive vaginal films based on HPMC and zein as novel formulations to prevent sexual transmission of HIV. *Int. J. Pharm.* **2019**, *570*, 118643. [\[CrossRef\]](#)
62. Mamani, P.L.; Ruiz-Caro, R.; Veiga, M.D. Matrix Tablets: The Effect of Hydroxypropyl Methylcellulose/Anhydrous Dibasic Calcium Phosphate Ratio on the Release Rate of a Water-Soluble Drug Through the Gastrointestinal Tract I. In Vitro Tests. *AAPS PharmSciTech* **2012**, *13*, 1073–1083. [\[CrossRef\]](#)
63. Owen, D.H.; Katz, D.F. A review of the physical and chemical properties of human semen and the formulation of a semen simulant. *J. Androl.* **2005**, *26*, 459–469. [\[CrossRef\]](#)
64. Shah, V.P.; Tsong, Y.; Sathe, P.; Liu, J.P. In vitro dissolution profile comparison- Statistics and analysis of the similarity factor, *f*₂. *Pharm. Res.* **1998**, *15*, 889–896. [\[CrossRef\]](#)

65. Harada, S.; Koyanagi, Y.; Yamamoto, N. Infection of HTLV-III/LAV in HTLV-I-carrying cells MT-2 and MT-4 and application in a plaque assay. *Science* **1985**, *229*, 563–566. [[CrossRef](#)]
66. Krug, H.F. *Handbook Standard Procedures for Nanoparticle Testing*; Comprehensive Assessment of Hazardous Effects of Engineering Nanomaterials on the Immune System Quality; EMPA: Dübendorf, Switzerland, 2011; p. 225.



© 2020 by the authors. Licensee MDPI, Basel, Switzerland. This article is an open access article distributed under the terms and conditions of the Creative Commons Attribution (CC BY) license (<http://creativecommons.org/licenses/by/4.0/>).